

1    **The *Rhodobacter sphaeroides* methionine sulfoxide reductase MsrP can reduce *R*- and *S*-**  
2    **diastereomers of methionine sulfoxide from a broad-spectrum of protein substrates.**

3

4    Lionel Tarrago<sup>1,\*</sup>, Sandrine Grosse<sup>1</sup>, Marina I. Siponen<sup>1</sup>, David Lemaire<sup>2</sup>, Béatrice Alonso<sup>1</sup>,  
5    Guylaine Miotello<sup>3</sup>, Jean Armengaud<sup>3</sup>, Pascal Arnoux<sup>1</sup>, David Pignol<sup>1</sup>, Monique Sabaty<sup>1,\*</sup>

6

7    <sup>1</sup> Laboratoire de Bioénergétique Cellulaire, UMR 7265, Aix Marseille Univ, CEA, CNRS,  
8    BIAM, Saint Paul-Lez-Durance, France.

9    <sup>2</sup> Laboratoire des Interactions Protéine-Métal, UMR 7265, Aix Marseille Univ, CEA, CNRS,  
10   BIAM, Saint Paul-Lez-Durance, France.

11   <sup>3</sup> Laboratoire Innovations technologiques pour la Détection et le Diagnostic (Li2D), Service de  
12   Pharmacologie et Immunoanalyse (SPI), CEA, INRA, F-30207 Bagnols sur Cèze, France.

13   \* Correspondence: [lioneltarrago@msn.com](mailto:lioneltarrago@msn.com) (L. T.) or [monique.sabaty@cea.fr](mailto:monique.sabaty@cea.fr) (M. S.)

## 14 **Summary**

15 Methionine (Met) is prone to oxidation and can be converted to Met sulfoxide (MetO), which  
16 exists as *R*- and *S*-diastereomers. MetO can be reduced back to Met by the ubiquitous  
17 methionine sulfoxide reductase (Msr) enzymes. Canonical MsrA and MsrB were shown as  
18 absolutely stereospecific for the reduction of *S*- and *R*-diastereomer, respectively. Recently, the  
19 molybdenum-containing protein MsrP, conserved in all gram-negative bacteria, was shown to  
20 be able to reduce MetO of periplasmic proteins without apparent stereospecificity in  
21 *Escherichia coli*. Here, we describe the substrate specificity of the *Rhodobacter sphaeroides*  
22 MsrP. Proteomics analysis coupled to enzymology approaches indicate that it reduces a broad  
23 spectrum of periplasmic oxidized proteins. Moreover, using model proteins, we demonstrated  
24 that RsMsrP preferentially reduces unfolded oxidized proteins and we confirmed that this  
25 enzyme, like its *E. coli* homolog, can reduce both *R*- and *S*-diastereomers of MetO with similar  
26 efficiency.

## 27 **Introduction**

28           Aerobic life exposes organisms to reactive oxygen species (ROS) derived from  
29 molecular oxygen, such as hydrogen peroxide (H<sub>2</sub>O<sub>2</sub>) or singlet oxygen (<sup>1</sup>O<sub>2</sub>). Bioenergetics  
30 chains are important sources of intracellular ROS, with H<sub>2</sub>O<sub>2</sub> principally produced during  
31 respiration (Messner and Imlay, 1999) and <sup>1</sup>O<sub>2</sub> arising from photosynthesis (Glaeser et al.,  
32 2011). These oxidative molecules act as signaling messengers playing major roles in numerous  
33 physiological and pathological states in most organisms and their production and elimination  
34 are tightly regulated (Ezraty et al., 2017). However, numerous stresses can affect ROS  
35 homeostasis and increase their intracellular concentration up to excessive values leading to  
36 uncontrolled reactions with sensitive macromolecules (Imlay, 2013). For instance,  
37 photosynthetic organisms, such as plants or the purple bacteria *Rhodobacter sphaeroides* can  
38 experience photo-oxidative stress in which unbalance between incident photons and electron  
39 transfer in photosynthesis generates detrimental accumulation of <sup>1</sup>O<sub>2</sub> (Ziegelhoffer and  
40 Donohue, 2009). Moreover, production of ROS could be used advantageously in a defensive  
41 strategy against potential pathogenic invaders. For instance, neutrophils produce the strong  
42 oxidant hypochlorite (ClO<sup>-</sup>) from H<sub>2</sub>O<sub>2</sub> and chlorine ions to eliminate bacteria and fungi (Ezraty  
43 et al., 2017). Because of their abundance in cells, proteins are the main targets of oxidation  
44 (Davies, 2005). Methionine (Met) is particularly prone to oxidation and the reaction of Met  
45 with oxidant leads to the formation of Met sulfoxide (MetO), which exists as two diastereomers  
46 *R* (Met-*R*-O) and *S* (Met-*S*-O), and further oxidation can form Met sulfone (MetO<sub>2</sub>) (Sharov et  
47 al., 1999; Vogt, 1995). Contrary to most oxidative modifications on amino acids, the formation  
48 of MetO is reversible, and oxidized proteins can be repaired thanks to methionine sulfoxide  
49 reductases (Msr) enzymes that exist principally in two types, MsrA and MsrB. These enzymes,  
50 present in almost all organisms, did not evolve from a common ancestor gene and possess an  
51 absolute stereospecificity toward their substrates. Indeed, MsrA can reduce only Met-*S*-O (Ejiri

52 et al., 1979; Lowther et al., 2002; Moskovitz et al., 2002; Sharov et al., 1999; Vieira Dos Santos  
53 et al., 2005) whereas MsrB acts only on Met-*R*-O (Grimaud et al., 2001; Kumar et al., 2002;  
54 Lowther et al., 2002; Moskovitz et al., 2002; Vieira Dos Santos et al., 2005). This strict  
55 stereospecificity was enzymatically demonstrated using Met-*R*-O and Met-*S*-O chemically  
56 prepared from racemic mixtures of free MetO or using HPLC methods allowing discrimination  
57 of both diastereomers, and was structurally explained by deciphering the mirrored pictures of  
58 their active site, in which only one MetO diastereomer can be accommodated (Lowther et al.,  
59 2002). While MsrA can reduce Met-*S*-O, whether as a free amino acid or included in proteins,  
60 MsrB is specialized in the reduction of protein-bound Met-*R*-O, and both are more efficient on  
61 unfolded oxidized proteins (Tarrago et al., 2012; Tarrago and Gladyshev, 2012). Eukaryotic  
62 Msrs are important actors in oxidative stress protection, aging and neurodegenerative diseases  
63 in animals (Kim, 2013), and during environmental stresses or seed longevity in plants  
64 (Châtelain et al., 2013; Laugier et al., 2010). In bacteria, MsrA and MsrB are generally located  
65 in the cytoplasm (Ezraty et al., 2017), except for *Neisseria* or *Streptococcus* species, for which  
66 MsrA and MsrB enzymes can be addressed to the envelope (Saleh et al., 2013; Skaar et al.,  
67 2002). They play a role in the protection against oxidative stress and as virulence factors (Ezraty  
68 et al., 2017).

69         Beside these stereotypical MSRs found in all kind of organisms, several bacterial  
70 molybdenum cofactor-containing enzymes can reduce MetO. Particularly, the biotin sulfoxide  
71 reductase BisC, or its homolog TorZ/BisZ, specifically reduce the free form of Met-*S*-O, in  
72 *Escherichia coli* cytoplasm (Ezraty et al., 2005) and *Haemophilus influenza* periplasm,  
73 respectively (Dhouib et al., 2016). Moreover, *E. coli* DMSO reductase reduce a broad spectrum  
74 of substrates, among which MetO (Weiner et al., 1988), and the *R. sphaeroides* homolog was  
75 shown as absolutely stereospecific towards *S*-enantiomer of several alkyl aryl sulfoxides (Abo  
76 et al., 1995). Finally, another molybdoenzyme, MsrP (formerly known as YedY), was recently

77 identified as a key player of MetO reduction in the periplasm (Gennaris et al., 2015; Melnyk et  
78 al., 2015). MsrP was shown to be induced by exposure to the strong oxidant hypochlorite (ClO<sup>-</sup>  
79 ) and to reduce MetO on several abundant periplasmic proteins in *E. coli* (Gennaris et al., 2015)  
80 or on a Met-rich protein in *Azospira suillum* (Melnyk et al., 2015). A most striking feature of  
81 the *E. coli* MsrP (EcMsrP) is that, contrary to all known methionine sulfoxide reductases, it  
82 seems capable of reducing both Met-*R*-O and Met-*S*-O (Gennaris et al., 2015). The cistron,  
83 *msrP*, belongs to an operon together with the cistron encoding the transmembrane protein  
84 MsrQ, which is responsible for the electron transfer to MsrP from the respiratory chain. The  
85 operon is conserved in the genome of most gram-negative bacteria suggesting that the MsrP/Q  
86 system is very likely a key player for the general protection of the bacterial envelope against  
87 deleterious protein oxidation (Gennaris et al., 2015; Melnyk et al., 2015). *R. sphaeroides* MsrP  
88 (RsMsrP) shares 50% identical amino acids residues with EcMsrP and transcriptomic analyses  
89 evidenced that *RsmsrP* is strongly induced under high-light conditions, suggesting a putative  
90 role in protecting the periplasm against <sup>1</sup>O<sub>2</sub> (Glaeser et al., 2007).

91 In this paper, we describe the biochemical characterization of RsMsrP regarding its  
92 substrate specificity. Using kinetics activity experiments and mass spectrometry analysis, we  
93 show that RsMsrP is a very efficient protein-bound MetO reductase, which lacks  
94 stereospecificity and preferentially acts on unfolded oxidized proteins. Proteomics analysis  
95 indicate that it can reduce a broad spectrum of proteins in *R. sphaeroides* periplasm, and that  
96 Met sensitive to oxidation and efficiently reduced by RsMsrP are found in clusters and in  
97 specific amino acids sequences.

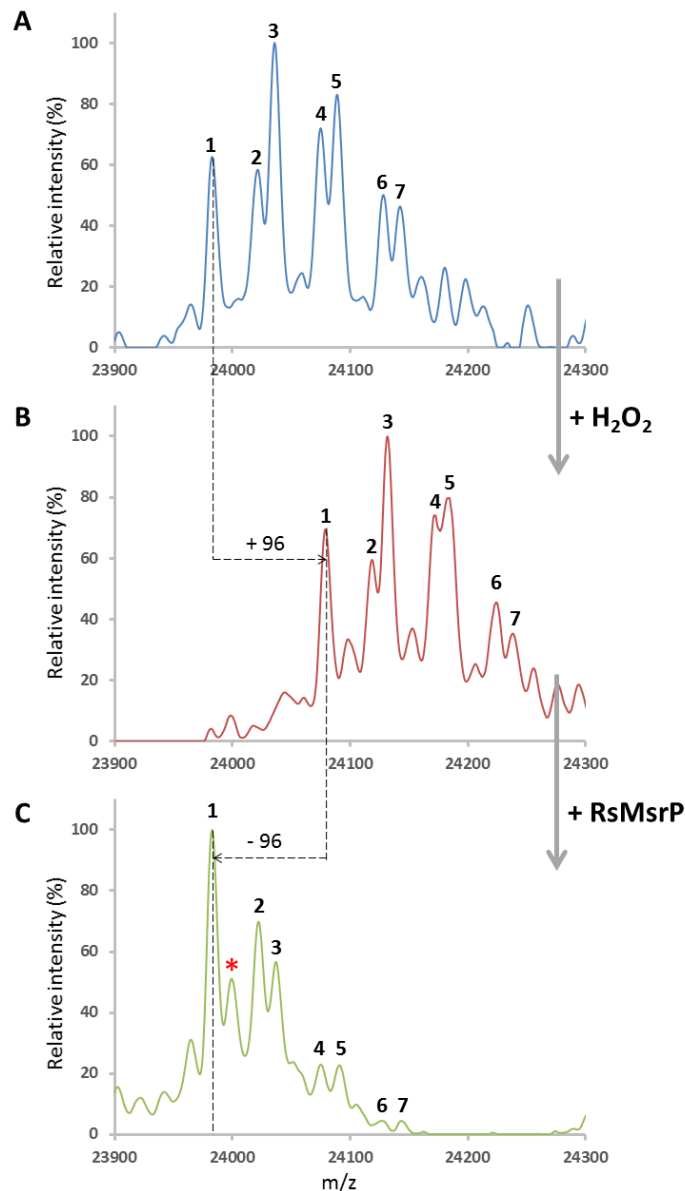
## 98 **Results**

### 99 *The R. sphaeroides MsrP is an efficient protein-MetO reductase*

100           The results showing that the EcMsrP is a protein-bound MetO reductase, able to reduce  
101 both *R*- and *S*-diastereomer of MetO (Gennaris et al., 2015) prompted us to evaluate whether  
102 these properties are conserved for RsMsrP. As the EcMsrP was determined to be 5-fold less  
103 efficient to reduce the Met-*S*-O than Met-*R*-O, and knowing that all previously identified MetO  
104 reductases were absolutely stereospecific toward one enantiomer, we thought that it cannot be  
105 excluded that a protein contamination might explain the apparent ability of the EcMsrP to  
106 reduce the Met-*S*-O (Gennaris et al., 2015). Such potential Met-*S*-O reductase contaminant  
107 should be able to use benzyl viologen (BV) as electron provider and one good candidate is the  
108 periplasmic DMSO reductase (Abo et al., 1995; Weiner et al., 1988). Thus, we prepared the  
109 recombinant RsMsrP from a *R. sphaeroides* strain devoid of the *dorA* gene encoding the  
110 catalytic subunit of the DMSO reductase (Sabaty et al., 2013). After purification on Ni-affinity  
111 column and removal of the polyhistidine tag, the mature enzyme was purified by gel filtration,  
112 then by strong anion exchange, yielding a highly pure enzyme (Figure S1).

113           After optimal pH determination (Figure S2), we determined the kinetics parameters of  
114 RsMsrP using BV as electron provider and several model substrates: the free amino acid MetO,  
115 a synthetic tripeptide Ser-MetO-Ser and the oxidized bovine  $\beta$ -casein (Table 1). The  $\beta$ -casein  
116 contains 6 Met, it is intrinsically disordered, and was shown as efficient substrate for the yeast  
117 MsrA and MsrB, after oxidation (Tarrago et al., 2012), see also Figure S3). Commercial  
118  $\beta$ -casein contains a mixture of genetic variants, appearing as multiple peaks on mass  
119 spectrometry (MS) spectra (Figure 1A). After oxidation with H<sub>2</sub>O<sub>2</sub>, MS analysis confirmed an  
120 increase in mass of 96 Da for each peak, very likely corresponding to the addition of 6 oxygen  
121 atoms on the Met residues (Figure 1B). Using the free MetO, we determined a  $k_{cat}$  of  $\sim 122$  s<sup>-1</sup>

122 and a  $K_M$  of  $\sim 115,000 \mu\text{M}$ , yielding a catalytic efficiency ( $k_{cat}/K_M$ ) of  $\sim 1,000 \text{ M}^{-1} \cdot \text{s}^{-1}$  (Table 1).  
123 With the Ser-MetO-Ser peptide, the  $k_{cat}$  and the  $K_M$  values were  $\sim 108 \text{ s}^{-1}$  and  $\sim 13,000 \mu\text{M}$ , and  
124 thus the  $k_{cat}/K_M$  was  $\sim 8,300 \text{ M}^{-1} \cdot \text{s}^{-1}$ . Compared to the free MetO, the  $\sim 8$ -fold increase in  
125 catalytic efficiency is due to the lower  $K_M$ , and thus this indicates that the involvement of the  
126 MetO in peptide bonds increases its ability to be reduced by the RsMsrP. With the oxidized  
127  $\beta$ -casein, the  $k_{cat}$  and the  $K_M$  were  $\sim 100 \text{ s}^{-1}$  and  $\sim 90 \mu\text{M}$ , respectively. The  $k_{cat}/K_M$  was thus  $\sim$   
128  $1,000,000 \text{ M}^{-1} \cdot \text{s}^{-1}$ . This value, 4 orders of magnitude higher than the one determined with the  
129 free MetO, indicates that the oxidized protein is a far better substrate for the RsMsrP. Moreover,  
130 even assuming that all MetO in the oxidized  $\beta$ -casein were equal substrates for the RsMsrP and  
131 thus multiplying the  $K_M$  by 6, the catalytic efficiency obtained ( $\sim 175,000 \text{ M}^{-1} \cdot \text{s}^{-1}$ ) remained  $\sim$   
132 175-fold higher for the oxidized protein than for the free amino acid. These results indicated  
133 that the RsMsrP acts effectively as a protein-MetO reductase.



134

135 **Figure 1. Mass spectrometry spectrum of  $\beta$ -casein non-oxidized (A), oxidized with H<sub>2</sub>O<sub>2</sub>**  
136 **(B) and repaired by RsMsRP (C).** A) Commercial  $\beta$ -casein exists as mixture of genetic  
137 variants (7 in our batch).  $\beta$ -casein was analyzed by ESI-MS. Main peaks masses: 1, 23982.7  
138 Da; 2, 24021.6 Da; 3, 24035.9 Da; 4, 24075.0 Da; 5, 24089.1 Da; 6, 24127.5 Da; 7, 24142.5  
139 Da. B)  $\beta$ -casein was oxidized with 50 mM H<sub>2</sub>O<sub>2</sub> before MS analysis. All major peaks undergone  
140 an increase of ~ 96 Da compared to the non-oxidized sample. Main peaks masses: 1, 24079.1  
141 Da; 2, 24118.5 Da; 3, 24131.8 Da; 4, 24172.2 Da; 5, 24184.3 Da; 6, 24224.4 Da; 7, 24238.2  
142 Da. C) Oxidized  $\beta$ -casein was incubated with RsMsRP (25 nM) in presence of BV (0.8 mM)  
143 and sodium dithionite (2 mM) as electron donors. All major peaks had masses corresponding  
144 of the non-oxidized  $\beta$ -casein, showing the ability to reduce all MetO in this protein. Note the  
145 presence of a peak with an increase of 16 Da (\*, mass of 23999,4 Da) compared to the main  
146 reduced peak, indicating an incomplete reduction of the total protein pool. Main peaks masses:  
147 1, 23983.0 Da; 2, 24022.4 Da; 3, 24037.1 Da; 4, 24075.0 Da; 5, 24091.0 Da; 6, 24128.2 Da; 7,  
148 24143.7 Da.

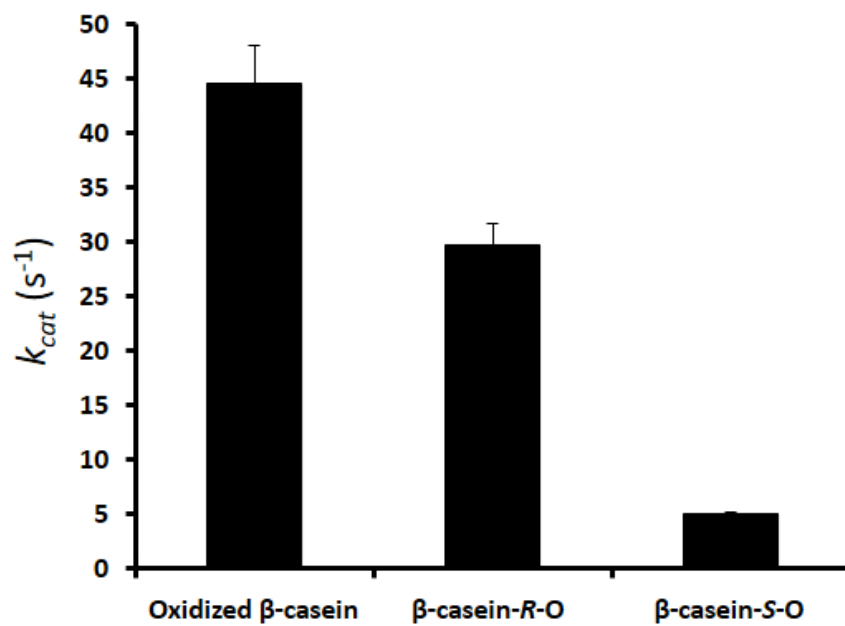


149 *RsMsrP reduces both Met-R-O and Met-S-O of an oxidized model protein*

150 To determine whether the RsMsrP can reduce both MetO diastereomers, we chose the  
151 oxidized bovine  $\beta$ -casein as model substrate because it was efficiently reduced by the yeast  
152 MsrA and MsrB indicating the presence of both *R* and *S* diastereomers of MetO (Tarrago et al.,  
153 2012). After oxidation with H<sub>2</sub>O<sub>2</sub>, we treated the protein with the MsrA and MsrB, taking  
154 advantage of their stereospecificity, to obtain protein samples containing only the Met-*R*-O  
155 (“ *$\beta$ -casein-R-O*”) or the Met-*S*-O (“ *$\beta$ -casein-S-O*”), respectively. The absence of one or the  
156 other diastereomer of MetO was validated by the absence of remaining Msr activity (Figure  
157 S3). These three forms containing two or only one diastereomer of MetO were tested as  
158 substrate for RsMsrP (Figure 2). We measured a  $k_{cat}$  of  $\sim 45$  s<sup>-1</sup> with the oxidized  $\beta$ -casein,  
159 which decreased to  $\sim 30$  and to 5 s<sup>-1</sup> for the  $\beta$ -casein containing the *R* or the *S* sulfoxide,  
160 respectively. This result showed that the RsMsrP can reduce both diastereomers of MetO, but  
161 appeared 6-fold less efficient to reduce the Met-*S*-O than the Met-*R*-O.

162 From this result, we postulated that the RsMsrP should be able to reduce all MetO in the  
163 oxidized  $\beta$ -casein, as this protein was intrinsically disordered and thus all MetO were very likely  
164 accessible. We evaluated this hypothesis by mass spectrometry analysis. When incubated with  
165 the RsMsrP, the mass of the oxidized protein decreased of 96 Da, showing that all MetO were  
166 reduced (Figure 1C). Altogether, these results clearly showed that the RsMsrP was able to  
167 reduce both *R*- and *S*-diastereomers of MetO contained in the oxidized  $\beta$ -casein, and thus lacked  
168 stereospecificity.

169  
170  
171  
172  
173  
174  
175



176

177 **Figure 2. RsMsrP activity using oxidized  $\beta$ -casein,  $\beta$ -casein-*R*-O and  $\beta$ -casein-*S*-O as**  
178 **substrates.** The oxidized  $\beta$ -casein (100  $\mu$ M) containing both diastereomers of MetO, only the  
179 *R* one (“ $\beta$ -casein-*R*-O”), or only the *S* one (“ $\beta$ -casein-*S*-O”) were assayed as substrate of  
180 RsMsrP. Data presented are average of 3 replicates.  $\pm$  S.D.

181 *The RsMsrP preferentially reduces Met-R-O but acts effectively on Met-S-O too*

182 To gain insight into the substrate preference of RsMsrP toward one of the diastereomers  
183 of MetO, we performed kinetics analysis using the oxidized  $\beta$ -casein containing the *R* or *S*  
184 diastereomers of MetO (Table 1; Figure S4). With the protein containing only the *R*-  
185 diastereomer of MetO (" $\beta$ -casein-*R*-O"), we determined a  $k_{cat}$  of  $\sim 50 \text{ s}^{-1}$ , a  $K_M$  of  $\sim 50 \mu\text{M}$  and  
186 thus a catalytic efficiency of  $\sim 950,000 \text{ M}^{-1} \cdot \text{s}^{-1}$ . In the case of the protein containing only the  
187 Met-*S*-O (" $\beta$ -casein-*S*-O"), the  $k_{cat}$  and  $K_M$  were  $\sim 8 \text{ s}^{-1}$  and of  $\sim 50 \mu\text{M}$ , respectively. This  
188 yielded a catalytic efficiency of  $142,000 \text{ M}^{-1} \cdot \text{s}^{-1}$ . This value,  $\sim 7$  fold lower than the one obtained  
189 with the  $\beta$ -casein-*R*-O, was due to the lower  $k_{cat}$  as the  $K_M$  was not changed. These values seem  
190 to indicate that the RsMsrP preferentially reduced the *R* than the *S* diastereomer of MetO in the  
191 oxidized  $\beta$ -casein. However, as we could not exclude that the proportion of Met-*R*-O was higher  
192 than the proportion of Met-*S*-O in the protein, we developed an assay to estimate the number  
193 of MetO reduced by the RsMsrP in the three forms of oxidized  $\beta$ -casein. We measured the total  
194 moles of BV consumed for the reduction of all MetO using subsaturating concentrations of the  
195 oxidized protein. Practically, the absorbance at 600 nm was measured before and 90 min after  
196 the addition of the substrate. As two moles of BV are consumed per mole of MetO reduced, we  
197 obtained the apparent stoichiometry of RsMsrP toward the oxidized protein by determining the  
198 slope of the linear regression of the straight defined by the amount of MetO reduced as a  
199 function of substrate concentration (Figure S5). The values determined were  $\sim 4.6$ ,  $\sim 3.2$  and  $\sim$   
200 1.8 for the oxidized  $\beta$ -casein, the  $\beta$ -casein-*R*-O and the  $\beta$ -casein-*S*-O, respectively. In the case  
201 of the oxidized  $\beta$ -casein, we expected a value of 6 based on the data obtained by mass  
202 spectrometry (Figure 1). This may have been due to the heterogeneity of the oxidized  $\beta$ -casein  
203 (all Met were not fully oxidized initially) and/or to a too short time of incubation (all MetO  
204 were not fully reduced, as indicated by the presence of a peak corresponding to a portion of  
205  $\beta$ -casein not fully reduced in Figure 1C). To compare the catalytic parameters, the data were

206 normalized by multiplying the  $K_M$  by these apparent stoichiometries, yielding values per MetO  
207 reduced and thus allowing the removal of variation due to the different numbers of Met-*R*-O or  
208 Met-*S*-O reduced. The catalytic efficiencies were thus 230,000, 300,000 and 80,000  $M^{-1}\cdot s^{-1}$  for  
209 the oxidized  $\beta$ -casein, the  $\beta$ -casein-*R*-O and the  $\beta$ -casein-*S*-O, respectively (Table 1). The  
210 highest value was thus those obtained for the  $\beta$ -casein containing only the *R* form of MetO,  
211 indicating that this diastereomer was the preferred substrate for the RsMsP. However, the value  
212 obtained with the  $\beta$ -casein-*S*-O was only less than 4-fold lower, showing that the RsMsP can  
213 also act effectively on the Met-*S*-O.

214

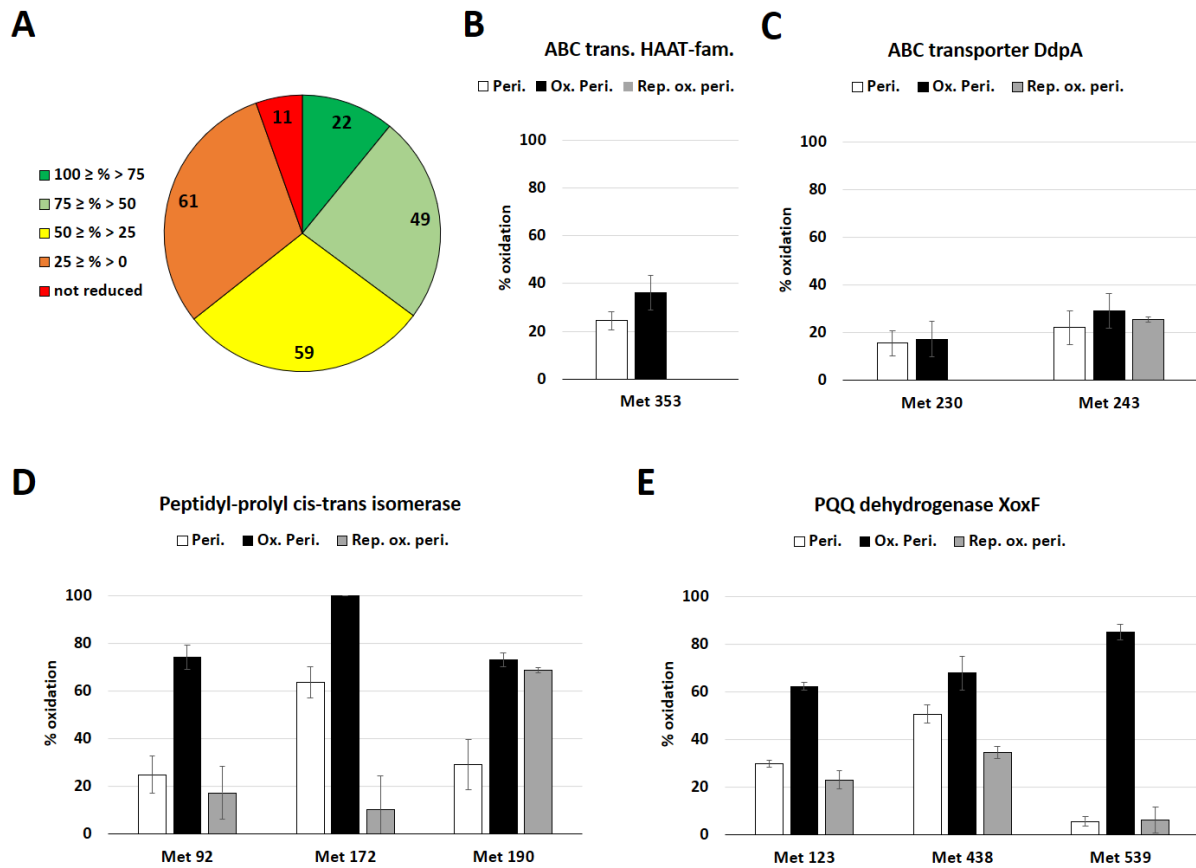
#### 215 *RsMsP can reduce a broad spectrum of periplasmic proteins*

216 To identify potential periplasmic substrates of RsMsP and gain insight into its substrate  
217 specificity, we applied a high-throughput shotgun proteomic strategy. Periplasmic proteins  
218 from *msrP* *R. sphaeroides* mutant were extracted, oxidized with NaOCl and then reduced *in*  
219 *vitro* with the recombinant RsMsP. Untreated periplasmic proteins, oxidized periplasmic  
220 proteins and RsMsP-treated oxidized periplasmic proteins were analyzed by semi-quantitative  
221 nanoLC–MS/MS. All experiments were done systematically for 3 biological replicates and  
222 resulted in the identification of 362,700 peptide-to-spectrum matches. From all the 11,320  
223 individual peptide sequences, we identified 2,553 unique Met belonging to 720 proteins. The  
224 overall percentage of Met oxidation were ~ 35%, ~ 71% and ~ 40% for proteins from the  
225 periplasm extract, the oxidized periplasm extract and the RsMsP-repaired proteins,  
226 respectively (Table S1). This first result indicates that the RsMsP is very likely able to reduce  
227 MetO from numerous proteins and to restore an oxidation rate similar to that of the periplasmic  
228 extract that has not undergone any oxidation.

229 The identification of preferential RsMsrP substrates requires the precise comparison of  
230 the oxidation state of Met residues from periplasmic proteins before and after the action of the  
231 enzyme. After tryptic digestion, since most of the Met/MetO-containing peptides were found  
232 in low abundance (*i.e.* with very low spectral counts), we focused on the proteins robustly  
233 detected in all samples. We selected the Met-containing peptides for which at least 10 spectral  
234 counts were detected in two replicates for each condition (*i.e.* untreated periplasm, oxidized  
235 periplasm and repaired oxidized periplasm) and at least 7 spectral counts were found in the third  
236 replicate. This restricted the dataset to 202 unique Met belonging to 70 proteins ([Table S2](#)).  
237 Overall percentage of Met oxidation (calculated as the number of spectral counts for a MetO-  
238 containing peptide vs. the total number of spectral count for this peptide) varied from 2% to  
239 87%, from 9% to 100% and from 4% to 91% in periplasm, oxidized periplasm and repaired  
240 oxidized periplasm, respectively. Comparison of Met-O containing peptides between oxidized  
241 and RsMsrP treated samples indicates that the percentage of reduction varied from 100 % to no  
242 reduction at all. 11 MetO were not reduced and 22 were reduced at more than 75 % (only 2 at  
243 100 %). The percentage of reduction for the remaining majority of MetO was almost distributed  
244 uniformly between inefficient (less than 25 %) to efficient (75% or more) reduction ([Figure](#)  
245 [3A](#)).

246 No clear evidence of sequence or structure characteristic arose from these 70 identified  
247 proteins, neither in term of size or in Met content ([Table S2](#)). The periplasmic chaperone SurA,  
248 the peptidyl-prolyl cis-trans isomerase PpiA, the thiol-disulfide interchange protein DsbA, the  
249 spermidine/putrescine-binding periplasmic protein PotD and the ProX protein were previously  
250 proposed as potential substrates of the EcMsrP ([Gennaris et al., 2015](#)). All these proteins  
251 contain at least one MetO among the most efficiently reduced by the RsMsrP ([Table S2](#)),  
252 indicating that they are potential conserved substrates of MsrP enzymes in *E. coli* and *R.*  
253 *sphaeroides*, and very likely in numerous gram-negative bacteria.

254           The sensibility to oxidation of the Met belonging to these 70 proteins, and their  
255 efficiency of reduction by the RsMsP show a wide range of variation, from Met highly  
256 sensitive to oxidation and efficiently reduced to Met barely sensitive to NaOCl treatment and  
257 not reduced by RsMsP (Table S2). Moreover, this diversity could be visible within a single  
258 protein, in which all Met may not be oxidized and reduced uniformly. For instance, the ABC  
259 transporter DdpA, along with another putative ABC transporter (Figure 3B and C), contained  
260 one of the two only MetO found as fully reduced in the dataset (Met 230 and Met353,  
261 respectively), although DdpA also contained the Met 243 that was neither efficiently oxidized  
262 or reduced. This is also illustrated by the case of the peptidyl-prolyl cis-trans isomerase, which  
263 possessed the Met found to have the higher decrease in oxidation in all the dataset (Met 172)  
264 but also a Met almost not reduced by the RsMsP (Met 190) (Figure 3D). The Met 539 of the  
265 PQQ dehydrogenase XoxF illustrates the case in which a Met was highly sensitive to NaOCl-  
266 oxidation and very efficiently reduced (Figure 3E). Twenty-one Met were oxidized at 50 % or  
267 more and reduced by 50 % or more by RsMsP (Table S2). Altogether, these results show that  
268 RsMsP can reduce a broad spectrum of apparently unrelated proteins (only 11 Met among 202  
269 were not reduced). However, since all MetO were not reduced with similar efficiency, some  
270 structural or sequence determinants could drive the ability of MetO to be reduced by the  
271 RsMsP.



272

273 **Figure 3. Characteristics of MetO reduction sites and oxidation state of Met in**  
 274 **representative proteins.** A) Repartition of the number of MetO per percentage of reduction by  
 275 RsMsrP. B) Percentage of oxidation of Met 353 of putative ABC transporter from HAAT  
 276 family in the 3 analyzed samples. C) Percentage of oxidation of Met 230 and 243 of ABC  
 277 transporter DdpA. D) Percentage of oxidation of Met 92, 172 and 190 in the peptidyl-prolyl  
 278 cis-trans isomerase. E) Percentage of oxidation of Met 123, 438 and 539 of the pyrroloquinoline  
 279 quinone (PQQ) dehydrogenase XoxF.

280

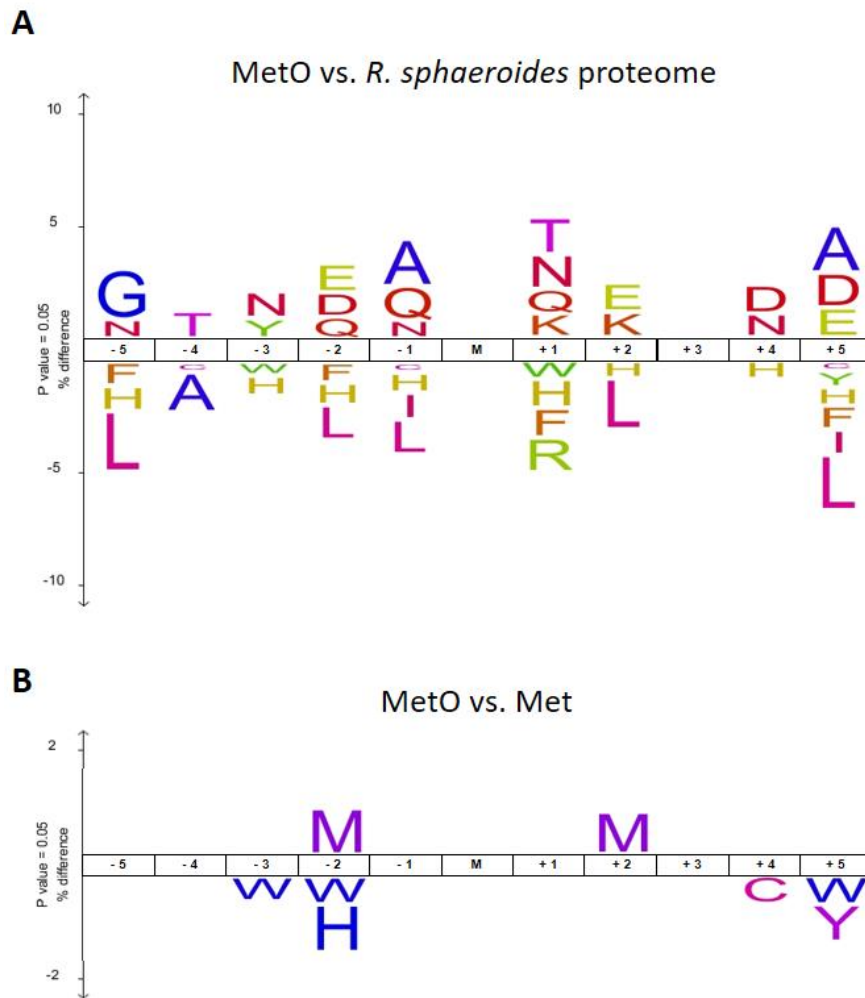
281 *The nature of the amino acids surrounding a MetO influences the RsMsrP efficiency*

282           Having in hands a relatively large dataset of oxidized and reduced Met prompted us to  
283 search for consensus sequences that could favor or impair the oxidation of a Met or the  
284 reduction of a MetO by the RsMsrP. For all identified Met, we extracted, the surrounding 5  
285 amino acids on the N- and C-terminal sides to obtain an 11-amino acid sequence with the  
286 considered Met centered at the 6<sup>th</sup> position. We then performed an IceLogo analysis aiming to  
287 identify whether some residues were enriched or depleted around the target Met. The principle  
288 is to compare a ‘positive’ dataset of peptides, to a ‘negative’ one (Colaert et al., 2009). To find  
289 potential consensus sequence of oxidation, we first compared all unique MetO-containing  
290 peptides from both the untreated and the NaOCl-oxidized periplasmic extracts, our positive  
291 dataset, to the theoretical *R. sphaeroides* proteome used as negative dataset. The IceLogo  
292 presented in Figure 4A shows that MetO-containing sequences were mainly depleted of His  
293 and aromatic or hydrophobic residues (Trp, Phe, Tyr, Leu, Ile) and were mainly enriched of  
294 polar or charged amino acids (Asn, Gln, Asp, Glu and Lys). This suggests that Met in a polar  
295 environment, as commonly found at the surface of proteins, are very likely more susceptible to  
296 oxidation than those located in hydrophobic environments as in the protein core. We then  
297 compared all these unique MetO-containing peptides to all the Met-containing peptides from  
298 the same samples (Figure 4B), and we observed that principally Trp, along with His, Tyr and  
299 Cys, were depleted around the potentially oxidized Met. Strikingly, the only amino acid  
300 significantly more abundant around an oxidized Met was another Met in position -2 and +2.  
301 These results indicate that oxidation sensitive Met might be found as clusters.

302

303





304

305 **Figure 4. IceLogo representation of enriched and depleted amino acids around site of Met**  
306 **oxidation.** A) Enrichment and depletion of amino acids around the oxidized Met (M) found in  
307 periplasmic extracts and oxidized periplasmic extracts by comparison with the theoretical  
308 proteome of *R. sphaeroides*. B) The same oxidized peptides were analyzed using the peptides  
309 containing a non-oxidized Met from the same samples (periplasm and oxidized periplasm  
310 extracts).

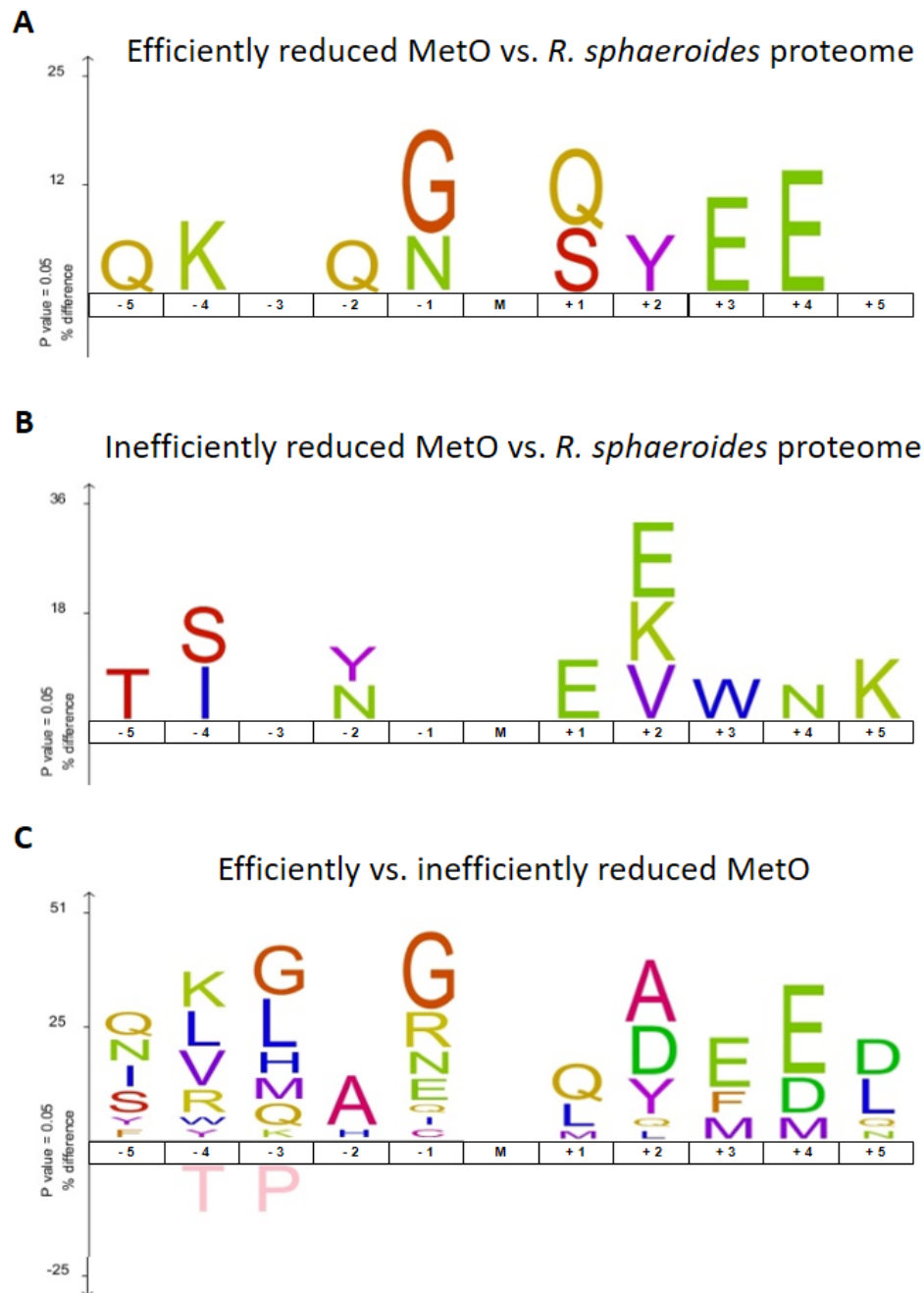
311 To identify potential consensus sequence favorable to MetO reduction by the RsMsRP,  
312 we performed a precise comparison of the percentage of oxidation before and after the action  
313 of the enzyme. We thus defined two criteria to characterize the reduction state of each Met: i)  
314 the percentage of reduction calculated using the formula described in [Table S2](#) and based on  
315 the comparison of the oxidation percentages in oxidized and repaired oxidized periplasm. For  
316 instance, a Met found oxidized at 25 % in the oxidized periplasm and at 5 % in the repaired  
317 oxidized periplasm was considered enzymatically reduced at 80 %. ii) the decrease in  
318 percentage of oxidation by comparison of the 2 samples. For instance, the same Met found  
319 oxidized at 25 % in the oxidized periplasm and 5 % in the repaired extract had a decrease in the  
320 percentage of oxidation of 20 %. This second criterion was used to avoid bias in which very  
321 little oxidized Met were considered as efficient substrate (*i.e.* a Met oxidized at 5 % in the  
322 oxidized periplasm extract and at 1 % in the repaired oxidized periplasm was reduced at 80 %,  
323 similarly to one passing from 100 % to 20 %, which intuitively appears as a better substrate  
324 than the previous one). We selected as efficiently and inefficiently reduced MetO those for  
325 which both criteria were higher than 50 % and lower than 10 %, respectively. The comparison  
326 of the sequences surrounding the efficiently reduced MetO to the theoretical proteome of *R.*  
327 *sphaeroides* showed no depletion of amino acid, but mainly enrichment of polar amino acids  
328 (Gln, Lys, and Glu) around the oxidized Met ([Figure 5A](#)). Similar analysis with the inefficiently  
329 reduced MetO indicated the enrichment of Thr and Ser in the far N-terminal positions (-5 and -  
330 4) and of a Tyr in position -2 ([Figure 5B](#)). The C-terminal positions (+ 1 to +5) were mainly  
331 enriched in charged amino acids (Gln, Lys, and Glu), similarly to efficiently reduced MetO.  
332 This apparent contradiction may indicate that the amino acids in C-terminal position of the  
333 considered MetO did not really influence the efficiency of RsMsRP but were observed simply  
334 because of the inherent composition of the overall identified peptides. We then compared the  
335 variation of amino acids composition of the MetO-containing peptides between both datasets,

336 using the inefficiently reduced MetO as negative dataset (Figure 5C). The results resembled  
337 those obtained by comparison with the entire theoretical proteome of the bacterium, *i.e.* most  
338 enriched amino acids were polar (Glu, Gln, Asp and Lys) at most extreme positions (-5, -4 and  
339 + 2 to + 5). Of note, the conserved presence of a Gly in position -1, and the presence of several  
340 other Met around the central Met. This potential enrichment of Met around an oxidation site is  
341 consistent with the result found for the sensibility of oxidation (Figure 4B), and indicates that  
342 potential clusters of MetO could be preferred substrates for RsMsRP. We found 16 peptides  
343 containing 2 or 3 MetO, reduced at more than 25 % by RsMsRP (Table S2). This was illustrated,  
344 for example, by the cell division coordinator CpoB which possesses two close Met residues (66  
345 and 69) highly reduced by the RsMsRP, or by the uncharacterized protein (YP\_353998.1) having  
346 4 clusters of MetO reduced by the RsMsRP (Table S2).

347 From this analysis, the only depleted amino acids appeared to be Thr and Pro in positions  
348 -4 and -3 (Figure 4C). To validate these results, we designed two peptides,  
349 QWGAGM(O)QAEED and TTPGYM(O)EEWNK, as representative of most efficiently and  
350 most inefficiently RsMsRP-reduced peptide-containing MetO, respectively. We used them as  
351 substrate to determine kinetics parameters of reduction by RsMsRP (Table 1; Figure S6). The  
352 results showed that the peptide QWGAGM(O)QAEED was efficiently reduced, with the  
353 highest  $k_{cat}$  value from all the substrates we tested ( $\sim 480 \text{ s}^{-1}$ ) and a  $K_M$  of  $\sim 4,500 \mu\text{M}$ . This  
354 yield a  $k_{cat}/K_M$  of  $\sim 100,000 \text{ M}^{-1}.\text{s}^{-1}$ , which is 2 order of magnitude higher than the one  
355 determined for the free MetO, and 10-fold lower than for the oxidized  $\beta$ -casein (Table 1). On  
356 the contrary, the peptide TTPGYM(O)EEWNK was not efficiently reduced by RsMsRP (Table  
357 1; Figure S6). Indeed, we could not determine the kinetics parameters as activity value curve  
358 never reached an inflection point using concentration as high as  $5,000 \mu\text{M}$ . The maximal  $k_{cat}$   
359 value was determined at  $\sim 70 \text{ s}^{-1}$  at  $5,000 \mu\text{M}$  of peptide, which is  $\sim 3.5$ -fold less than the one  
360 determined with the same concentration of the other peptide ( $\sim 250 \text{ s}^{-1}$ ) (Figure S2). These

361 results are in full agreement with the proteomics analysis and confirm that the nature of the  
362 amino acids surrounding a MetO in a peptide or a protein strongly influences its ability to be  
363 reduced by RsMsrP.

364



365

366 **Figure 5. IceLogo representation of enriched and depleted amino acids around site of**  
 367 **MetO reduction by RsMsrP.** A) Enrichment of amino acids in peptides centered on the MetO  
 368 for which the percentage of reduction and the decrease in percentage of oxidation were both  
 369 superior to 50 % by comparison with the theoretical proteome of *R. sphaeroides*. B) Enrichment  
 370 of amino acids from peptides centered on the MetO for which the percentage of reduction and  
 371 the decrease in percentage were inferior to 10 % by comparison with the theoretical proteome  
 372 of *R. sphaeroides*. C) Enrichment and depletion of amino acids from efficiently reduced MetO-  
 373 containing peptides (dataset used in A)) by comparison with inefficiently reduced MetO-  
 374 containing peptides (dataset used in B)).

375

376 *The RsMsrP preferentially reduces unfolded oxidized proteins*

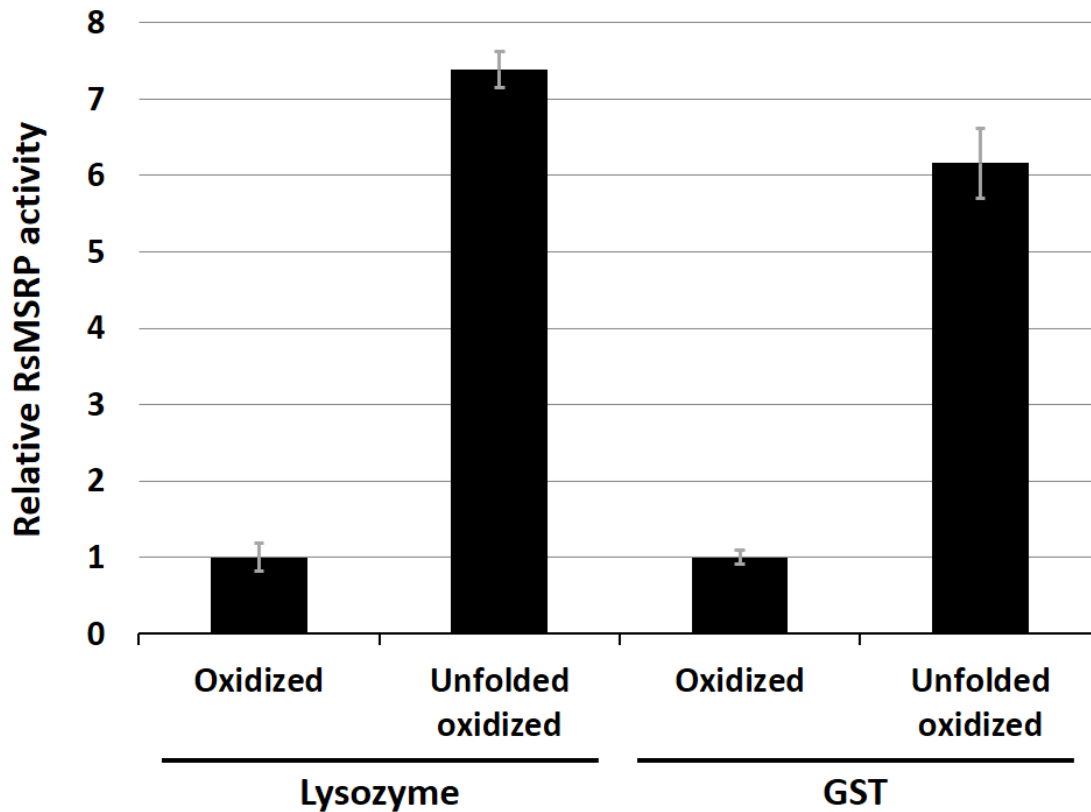
377 To test whether structural determinants affect RsMsrP efficiency of MetO reduction, we  
378 compared its activity using oxidized model proteins, either properly folded or unfolded. We  
379 started with the chicken lysozyme as it is a very well folded protein highly stabilized with four  
380 disulfide bonds (Ray et al., 2001). We oxidized it with H<sub>2</sub>O<sub>2</sub> and checked its oxidation state by  
381 mass spectrometry (Figure S7). Surprisingly, using a protocol similar to the one allowing the  
382 complete oxidation of the 6 Met of  $\beta$ -casein, we observed only a weak and incomplete oxidation  
383 of the protein. The major peak corresponded to the non-oxidized form and a small fraction had  
384 an increase of mass of 16 Da, likely corresponding to the oxidation of one Met. Nevertheless,  
385 we prepared from this oxidized sample, an unfolded oxidized lysozyme by reduction with  
386 dithiothreitol in 4M urea followed by iodoacetamide alkylation of cysteines, and both samples  
387 (oxidized and unfolded oxidized), were used as substrates for RsMsrP (Figure 6). We also used  
388 glutathione-S-transferase (GST) which possesses 9 Met and is highly structured. After  
389 oxidation with H<sub>2</sub>O<sub>2</sub>, GST was incubated with 4 M of the chaotropic agent urea, a concentration  
390 sufficient to induce complete unfolding of the protein (Tarrago et al., 2012). For both oxidized  
391 proteins, we observed a dramatic increase in activity after unfolding. Indeed, the RsMsrP  
392 activity increased 7-fold with the unfolded oxidized lysozyme compared to the folded one, and  
393 6-fold in the case of the unfolded oxidized GST compared to the folded oxidized GST (Figure  
394 6). As the unfolded oxidized protein solutions of lysozyme or GST contained a substantial  
395 amount of urea, we made controls in which the urea was added extemporaneously in the cuvette  
396 during the measurements, showing that urea did not influence the RsMsrP activity (Figure S8).

397 Mass spectrometry analysis showed that the RsMsrP was able to completely reduce the  
398 oxidized lysozyme in these conditions (Figure S7), suggesting that observed differences of  
399 repair between the folded- and unfolded-oxidized lysozyme were not due to the incapacity of  
400 the RsMSRP to reduce some MetO, but were due to kinetics parameters. We thus determined

401 the kinetic of reduction of these proteins by the RsMsrP (Table 1, Figure S8). With the oxidized  
402 lysozyme, the  $k_{cat}$  and the  $K_M$  were  $\sim 4 \text{ s}^{-1}$  and  $\sim 900 \text{ }\mu\text{M}$ , respectively. Using the unfolded  
403 oxidized lysozyme, the  $k_{cat}$  increased to  $\sim 7 \text{ s}^{-1}$  and the  $K_M$  decreased to  $\sim 100 \text{ }\mu\text{M}$ . The catalytic  
404 efficiency determined with the unfolded oxidized lysozyme was thus  $\sim 18$ -fold higher than the  
405 one determined using the oxidized lysozyme before unfolding ( $70,200 \text{ vs. } 4,000 \text{ M}^{-1} \cdot \text{s}^{-1}$ ).  
406 Similar results were obtained with the GST. Indeed, with the oxidized GST, we recorded  $k_{cat}$   
407 and  $K_M$  values of  $\sim 8 \text{ s}^{-1}$  and  $\sim 640 \text{ }\mu\text{M}$ , respectively whereas for the unfolded oxidized GST,  
408 the  $k_{cat}$  was slightly higher ( $\sim 12 \text{ s}^{-1}$ ), and the  $K_M$  was  $\sim 6$ -fold lower ( $\sim 100 \text{ }\mu\text{M}$ ). The catalytic  
409 efficiency was 10-fold higher for the unfolded oxidized GST than for its folded counterpart  
410 (Table 1; Figure S8). Altogether, these results showed that the RsMsrP is more efficient in  
411 reducing MetO in unfolded than in folded oxidized proteins. Moreover, as evidenced with  
412 lysozyme that contained only one MetO in our conditions, the increase in activity using  
413 unfolded substrate is not dependent of the number of MetO reduced.

414

415



416

417 **Figure 6. Relative RsMsrP activity using unfolded oxidized proteins.** The RsMsrP activity  
418 was determined as described in Figure S4. Oxidized and unfolded oxidized lysozyme were  
419 incubated at 100  $\mu\text{M}$  in 50 mM MES, pH 6.0. Initial turnover numbers were  $0.65 \pm 0.12 \text{ s}^{-1}$  and  
420  $7.38 \pm 0.23 \text{ s}^{-1}$  with oxidized and unfolded oxidized lysozyme, respectively. Activity with  
421 oxidized and unfolded oxidized GST (75  $\mu\text{M}$ ) was determined similarly except that reaction  
422 buffer was 30 mM Tris-HCl, pH 8.0 because unfolded oxidized GST precipitated in 50 mM  
423 MES, pH 6.0. Initial turnover numbers were  $0.86 \pm 0.08 \text{ s}^{-1}$  and  $5.31 \pm 0.39 \text{ s}^{-1}$  with oxidized  
424 and unfolded oxidized GST, respectively. Data presented are average of three replicates.  $\pm$  S.D.



## 425 Discussion

426 All organisms have to face harmful protein oxidation and almost all possess canonical  
427 Msrs that protect proteins by reducing MetO. Bacteria also have molybdoenzymes able to  
428 reduce MetO, as a free amino acid for the DMSO reductase (Weiner et al., 1988) or the biotin  
429 sulfoxide reductase BisC/Z (Dhouib et al., 2016; Ezraty et al., 2005), but also included in  
430 proteins in the case of the MsrP (Gennaris et al., 2015; Melnyk et al., 2015). Genetic studies  
431 and the conservation of MsrP in most gram-negative bacteria indicate that it is very likely a key  
432 player in the protection of periplasmic proteins against oxidative stress (Gennaris et al., 2015;  
433 Melnyk et al., 2015) However, an in-depth characterization of its protein substrate specificity  
434 is still lacking. In this work, we chose the MsrP from the photosynthetic purple bacteria *R.*  
435 *sphaeroides* as model enzyme to uncover such specificity. Using purified oxidized proteins and  
436 peptides, we showed that RsMsrP is a very efficient protein-containing MetO reductase, with  
437 apparent affinities ( $K_M$ ) for oxidized proteins 10 to 100-fold lower than for the tripeptide Ser-  
438 MetO-Ser or the free MetO (Table 1). As reported for canonical MsrA and MsrB (Tarrago et  
439 al., 2012), we observed important variations in the  $k_{cat}$  of reduction of different oxidized  
440 proteins, arguing for the existence of sequence and structural determinant affecting the enzyme  
441 efficiency (Table 1).

442 To find potential physiological substrates of RsMsrP and uncover their properties, we  
443 used a proteomic approach aiming to compare the oxidation state of periplasmic proteins after  
444 treatment with the strong oxidant NaOCl, then followed by RsMsrP reduction. We found 202  
445 unique Met, belonging to 70 proteins, for which the sensitivity of oxidation and the ability to  
446 serve as RsMsrP substrate varied greatly (Figure 3, Table S2). MetO efficiently reduced by  
447 RsMsrP belong to structurally and functionally unrelated proteins, indicating that RsMsrP very  
448 likely does not possess specific substrates and acts as a global protector of protein integrity in  
449 the periplasm. Interestingly, we observed from our IceLogo analysis that Met sensitive to

450 oxidation are generally presented in a polar amino acid environment and can be found in cluster  
451 (Figure 4). These properties might be common to all Met in proteins as similar results were  
452 found in human cells (Ghesquière et al., 2011; Hsieh et al., 2017) and plants (Jacques et al.,  
453 2015). Moreover, oxidized Met efficiently reduced by the RsMsP were also found in cluster in  
454 polar environment and our analysis shows that the presence of Thr and Pro in N-terminal side  
455 of a MetO strongly decrease RsMsP efficiency (Table 1, Figure 5 and S6). To our knowledge,  
456 the presence of a Thr close to a MetO was not previously shown to influence any Msr activity,  
457 but the presence of a Pro was shown to decrease or totally inhibit MetO reduction by the human  
458 MsrA and MsrB3, depending on its position (Ghesquière et al., 2011).

459 The presence of oxidation-sensitive Met efficiently reduced by the RsMsP in clusters  
460 on polar parts of proteins should facilitate the oxidation/reduction cycle aiming to scavenge  
461 ROS as previously proposed for canonical Msrs (Luo and Levine, 2009). This is also illustrated  
462 by the methionine-rich protein MrpX proposed as main substrate of the *A. suillum* MsP, which  
463 is almost only composed of Met, Lys, Glu and Asp (Melnyk et al., 2015). The presence of  
464 numerous MetO on a single molecule of protein substrate should increase the RsMsP  
465 efficiency as one molecule of substrate allows several catalytic cycles, potentially without  
466 breaking physical contact between the enzyme and its substrate.

467 Comparison of the RsMsP activity using folded or unfolded protein substrates  
468 (lysozyme and GST) showed that it is far more efficient to reduce unfolded oxidized proteins  
469 (Figure 6). Similar results were found for canonical Msrs (Tarrago et al., 2012). In the case of  
470 the MsrB it was because more MetO were accessible for reduction whereas for MsrA this  
471 increase was independent of the number of MetO reduced. Here, the use of the lysozyme  
472 containing only one MetO (Figure S7) undoubtedly showed that the increase in activity is not  
473 related to the unmasking of additional MetO upon protein denaturation (Table 1; Figure 6). This  
474 could indicate that the RsMsP has a better access to the MetO in the protein or that the MetO

475 is more easily accommodated in the active site of the enzyme because of increased flexibility.  
476 This should provide a physiological advantage to the bacteria during oxidative attacks, which  
477 could occur during other stresses such as acid or heat, hence promoting simultaneous oxidation  
478 and unfolding of proteins. Particularly, hypochlorous acid, shown to induce *msrP* expression in  
479 *E. coli* (Gennaris et al., 2015) and *A. suillum* (Melnyk et al., 2015) has strong oxidative and  
480 unfolding effect on target proteins (Winter et al., 2008).

481 Finally, previous work indicated that the *E. coli* MsrP lacks stereospecificity and can  
482 reduce both *R*- and *S*-diastereomers of MetO chemically isolated from a racemic mixture of free  
483 L-Met-*R,S*-O (Gennaris et al., 2015). This discovery is of fundamental importance as it breaks  
484 a paradigm in the knowledge about Met oxidation and reduction, and very likely for all  
485 enzymology as non-stereospecific enzymes were very rarely described. Indeed, to our  
486 knowledge, all previously characterized enzymes able to reduce Met sulfoxide or related  
487 substrates were shown as absolutely stereospecific. This was the case for the canonical MsrA  
488 and MsrB, which reduce only the *S*-diastereomer and the *R*-diastereomer, respectively (Ejiri et  
489 al., 1979; Grimaud et al., 2001; Kumar et al., 2002; Lowther et al., 2002; Moskovitz et al., 2002;  
490 Sharov et al., 1999; Vieira Dos Santos et al., 2005), as well as for the free Met-*R*-O reductase  
491 (Le et al., 2009; Lin et al., 2007) and for the molybdoenzymes DMSO reductase (Abo et al.,  
492 1995; Weiner et al., 1988) and BisC/Z (Dhouib et al., 2016; Ezraty et al., 2005). To evaluate  
493 the potential lack of stereospecificity of the RsMsrP, we chose to use a strategy different than  
494 the one used for *E. coli* MsrP (Gennaris et al., 2015) and prepared oxidized  $\beta$ -casein containing  
495 only one or the other MetO diastereomer using yeast MsrA and MsrB to eliminate the *S*- and  
496 the *R*-diastereomers, respectively. Activity assays and kinetics experiments using a highly  
497 purified RsMsrP demonstrated that it can efficiently reduce the  $\beta$ -casein containing only the *R*-  
498 or the *S*-diastereomer (Table 1; Figure 2 and S4). Moreover, this lack of stereospecificity was  
499 undoubtedly confirmed by the ability of the RsMsrP to reduce all 6 MetO formed on the

500 oxidized  $\beta$ -casein (Figure 1). These results, consistent with Gennaris and coworkers finding,  
501 indicate that this lack of stereospecificity is very likely common to all MsrP homologs. Together  
502 with the apparent ability of the enzyme to repair numerous unrelated oxidized proteins, the  
503 capacity to reduce both diastereomers of MetO, argues for a role of MsrP in the general  
504 protection of envelope integrity in gram negative bacteria. However, it raises questions  
505 regarding the structure of its active site as the enzyme should be able to accommodate both  
506 diastereomers. From this, we wondered whether the RsMsrP could reduce the Met sulfone,  
507 which can be imagined as a form of oxidized Met containing both *R*- and *S*-diastereomers, but  
508 we did not detect any activity (Figure S9). Although it could be because of an incompatibility  
509 in redox potential, it may indicate that this form of oxidized Met cannot reach the catalytic  
510 atom. The three-dimensional structure of the oxidized form of *E. coli* MsrP indicated that the  
511 molybdenum atom, which is supposed to be the catalytic center of the enzyme, is buried 16 Å  
512 from the surface of the protein (Loschi et al., 2004). The next challenge will be to understand  
513 the MsrP reaction mechanism and will require the determination of the enzyme structure in its  
514 oxidized and reduced forms bound to its MetO-containing substrates.

515

## 516 **Significance**

517 Protein quality control is a vital cellular process. The cell envelope and the periplasm of gram-negative  
518 bacteria are particularly exposed to oxidative molecules damaging proteins. Methionine residues are prone  
519 to oxidation, and can be converted to two diastereomers, *R* and *S*, of methionine sulfoxide (MetO). Almost  
520 all organisms possess the thiol-oxidoreductases, methionine sulfoxide reductases (Msr) A and B able to  
521 reduce the *S*- and *R*-MetO, respectively, with a strict stereospecificity. Recently, a new enzymatic system,  
522 MsrQ/MsrP which is conserved in all gram-negative bacteria, was identified as a key actor in the reduction  
523 of oxidized proteins in periplasm. The haem-binding membrane protein MsrQ transmits the reducing power  
524 coming from the electron transport chains to the molybdoenzyme MsrP which acts as protein-MetO  
525 reductase. MsrQ/MsrP function was genetically well established, but the identity and the biochemical  
526 properties of MsrP substrates remain unknown. In this work, using the purified MsrP enzyme from the  
527 photosynthetic bacteria *Rhodobacter sphaeroides* as a model, we show that it can reduce a broad spectrum  
528 of protein substrates. The most efficiently reduced MetO are found in cluster in amino acids sequence devoid  
529 of threonine and proline in C-terminal side. Moreover, *R. sphaeroides* MsrP lacks stereospecificity as it can  
530 reduce both *R* and *S* diastereomers of MetO, like its *Escherichia coli* homolog, and preferentially acts on  
531 unfolded oxidized proteins. Due to its high conservation of in all gram-negative, understanding how the  
532 MsrQ/MsrP system protects periplasmic proteins from oxidation and helps bacteria to cope with harmful  
533 environment is of fundamental importance and could provide insight to create molecules to fight pathogenic  
534 bacteria.

535

536 **Acknowledgments**

537 We are very grateful to Prof. Vadim, N. Gladyshev (Brigham's and Women Hospital and  
538 Harvard Medical School) for the gift of pET28a-MsrA, pET21b-MsrB, pET15b-TR1,  
539 pET15b-Trx1 and pGEX4T1 expression vectors. Pascaline Auroy-Tarrago (Laboratoire de  
540 Bioénergétique et Biotechnologie des Bactéries et Microalgues, CEA, BIAM) is acknowledged  
541 for her help with proteomics analysis. This work was supported by the Commissariat à l'Energie  
542 Atomique et aux Energies Alternatives (CEA) and by the project METOXIC (ANR 16-CE11-  
543 0012).

544

545 **Conflict of interest**

546 The authors declare no conflict of interest

547

548 **Author contributions**

549 LT, PA, DP and MS designed the study. LT, SG, MIS and MS purified RsMsrP. LT and MS  
550 prepared all other proteins. LT, SG, MIS, MS performed biochemical characterization of  
551 RsMsrP. LT, MS and DL performed  $\beta$ -casein and lysozyme mass spectrometry analysis and  
552 analyzed the data. SG and MS prepared *R. sphaeroides* 2.4.1 *msrP*<sup>-</sup> mutant and periplasmic  
553 proteins samples. BA, GM and JA performed proteomics analysis of periplasmic proteins and  
554 LT, MS, GM and JA analyzed the data. LT wrote the manuscript with contribution of DL, PA,  
555 DP, JA and MS. All authors approved the final manuscript.

## 556 References

- 557 Abo, M., Tachibana, M., Okubo, A., Yamazaki, S., 1995. Enantioselective deoxygenation of  
558 alkyl aryl sulfoxides by DMSO reductase from *Rhodobacter sphaeroides* f.s.  
559 *denitrificans*. *Bioorg. Med. Chem.* 3, 109–112. [https://doi.org/10.1016/0968-](https://doi.org/10.1016/0968-0896(95)00004-Z)  
560 [0896\(95\)00004-Z](https://doi.org/10.1016/0968-0896(95)00004-Z)
- 561 Châtelain, E., Satour, P., Laugier, E., Ly Vu, B., Payet, N., Rey, P., Montrichard, F., 2013.  
562 Evidence for participation of the methionine sulfoxide reductase repair system in plant  
563 seed longevity. *Proc. Natl. Acad. Sci. U. S. A.* 110, 3633–3638.  
564 <https://doi.org/10.1073/pnas.1220589110>
- 565 Colaert, N., Helsens, K., Martens, L., Vandekerckhove, J., Gevaert, K., 2009. Improved  
566 visualization of protein consensus sequences by iceLogo. *Nat. Methods* 6, 786–787.  
567 <https://doi.org/10.1038/nmeth1109-786>
- 568 Davies, M.J., 2005. The oxidative environment and protein damage. *Biochim. Biophys. Acta*  
569 1703, 93–109. <https://doi.org/10.1016/j.bbapap.2004.08.007>
- 570 Dhoub, R., Othman, D.S.M.P., Lin, V., Lai, X.J., Wijesinghe, H.G.S., Essilfie, A.-T., Davis,  
571 A., Nasreen, M., Bernhardt, P.V., Hansbro, P.M., McEwan, A.G., Kappler, U., 2016.  
572 A Novel, Molybdenum-Containing Methionine Sulfoxide Reductase Supports  
573 Survival of *Haemophilus influenzae* in an In vivo Model of Infection. *Front.*  
574 *Microbiol.* 7, 1743. <https://doi.org/10.3389/fmicb.2016.01743>
- 575 Ejiri, S.I., Weissbach, H., Brot, N., 1979. Reduction of methionine sulfoxide to methionine by  
576 *Escherichia coli*. *J. Bacteriol.* 139, 161–164.
- 577 Ezraty, B., Bos, J., Barras, F., Aussel, L., 2005. Methionine sulfoxide reduction and  
578 assimilation in *Escherichia coli*: new role for the biotin sulfoxide reductase BisC. *J.*  
579 *Bacteriol.* 187, 231–237. <https://doi.org/10.1128/JB.187.1.231-237.2005>
- 580 Ezraty, B., Gennaris, A., Barras, F., Collet, J.-F., 2017. Oxidative stress, protein damage and  
581 repair in bacteria. *Nat. Rev. Microbiol.* 15, 385–396.  
582 <https://doi.org/10.1038/nrmicro.2017.26>
- 583 Gennaris, A., Ezraty, B., Henry, C., Agrebi, R., Vergnes, A., Oheix, E., Bos, J., Leverrier, P.,  
584 Espinosa, L., Szewczyk, J., Vertommen, D., Iranzo, O., Collet, J.-F., Barras, F., 2015.  
585 Repairing oxidized proteins in the bacterial envelope using respiratory chain electrons.  
586 *Nature* 528, 409–412. <https://doi.org/10.1038/nature15764>
- 587 Ghesquière, B., Jonckheere, V., Colaert, N., Van Durme, J., Timmerman, E., Goethals, M.,  
588 Schymkowitz, J., Rousseau, F., Vandekerckhove, J., Gevaert, K., 2011. Redox  
589 proteomics of protein-bound methionine oxidation. *Mol. Cell. Proteomics MCP* 10,  
590 M110.006866. <https://doi.org/10.1074/mcp.M110.006866>
- 591 Glaeser, J., Nuss, A.M., Berghoff, B.A., Klug, G., 2011. Singlet oxygen stress in  
592 microorganisms. *Adv. Microb. Physiol.* 58, 141–173. [https://doi.org/10.1016/B978-0-](https://doi.org/10.1016/B978-0-12-381043-4.00004-0)  
593 [12-381043-4.00004-0](https://doi.org/10.1016/B978-0-12-381043-4.00004-0)
- 594 Glaeser, J., Zobawa, M., Lottspeich, F., Klug, G., 2007. Protein synthesis patterns reveal a  
595 complex regulatory response to singlet oxygen in *Rhodobacter*. *J. Proteome Res.* 6,  
596 2460–2471. <https://doi.org/10.1021/pr060624p>
- 597 Grimaud, R., Ezraty, B., Mitchell, J.K., Lafitte, D., Briand, C., Derrick, P.J., Barras, F., 2001.  
598 Repair of oxidized proteins. Identification of a new methionine sulfoxide reductase. *J.*  
599 *Biol. Chem.* 276, 48915–48920. <https://doi.org/10.1074/jbc.M105509200>
- 600 Hartmann, E.M., Allain, F., Gaillard, J.-C., Pible, O., Armengaud, J., 2014. Taking the  
601 shortcut for high-throughput shotgun proteomic analysis of bacteria. *Methods Mol.*  
602 *Biol. Clifton NJ* 1197, 275–285. [https://doi.org/10.1007/978-1-4939-1261-2\\_16](https://doi.org/10.1007/978-1-4939-1261-2_16)
- 603 Hsieh, Y.-J., Chien, K.-Y., Yang, I.-F., Lee, I.-N., Wu, C.-C., Huang, T.-Y., Yu, J.-S., 2017.  
604 Oxidation of protein-bound methionine in Photofrin-photodynamic therapy-treated



- 605 human tumor cells explored by methionine-containing peptide enrichment and  
606 quantitative proteomics approach. *Sci. Rep.* 7, 1370. <https://doi.org/10.1038/s41598-017-01409-9>
- 607
- 608 Imlay, J.A., 2013. The molecular mechanisms and physiological consequences of oxidative  
609 stress: lessons from a model bacterium. *Nat. Rev. Microbiol.* 11, 443–454.  
610 <https://doi.org/10.1038/nrmicro3032>
- 611 Jacques, S., Ghesquière, B., De Bock, P.-J., Demol, H., Wahni, K., Willems, P., Messens, J.,  
612 Van Breusegem, F., Gevaert, K., 2015. Protein Methionine Sulfoxide Dynamics in  
613 *Arabidopsis thaliana* under Oxidative Stress. *Mol. Cell. Proteomics MCP* 14, 1217–  
614 1229. <https://doi.org/10.1074/mcp.M114.043729>
- 615 Kim, H.-Y., 2013. The methionine sulfoxide reduction system: selenium utilization and  
616 methionine sulfoxide reductase enzymes and their functions. *Antioxid. Redox Signal.*  
617 19, 958–969. <https://doi.org/10.1089/ars.2012.5081>
- 618 Klein, G., Mathé, C., Biola-Clier, M., Devineau, S., Drouineau, E., Hatem, E., Marichal, L.,  
619 Alonso, B., Gaillard, J.-C., Lagniel, G., Armengaud, J., Carrière, M., Chédin, S.,  
620 Boulard, Y., Pin, S., Renault, J.-P., Aude, J.-C., Labarre, J., 2016. RNA-binding  
621 proteins are a major target of silica nanoparticles in cell extracts. *Nanotoxicology* 10,  
622 1555–1564. <https://doi.org/10.1080/17435390.2016.1244299>
- 623 Kumar, R.A., Koc, A., Cerny, R.L., Gladyshev, V.N., 2002. Reaction mechanism,  
624 evolutionary analysis, and role of zinc in *Drosophila* methionine-R-sulfoxide  
625 reductase. *J. Biol. Chem.* 277, 37527–37535. <https://doi.org/10.1074/jbc.M203496200>
- 626 Laugier, E., Tarrago, L., Vieira Dos Santos, C., Eymery, F., Havaux, M., Rey, P., 2010.  
627 *Arabidopsis thaliana* plastidial methionine sulfoxide reductases B, MSRBs, account  
628 for most leaf peptide MSR activity and are essential for growth under environmental  
629 constraints through a role in the preservation of photosystem antennae. *Plant J. Cell*  
630 *Mol. Biol.* 61, 271–282. <https://doi.org/10.1111/j.1365-313X.2009.04053.x>
- 631 Le, D.T., Lee, B.C., Marino, S.M., Zhang, Y., Fomenko, D.E., Kaya, A., Hacioglu, E., Kwak,  
632 G.-H., Koc, A., Kim, H.-Y., Gladyshev, V.N., 2009. Functional analysis of free  
633 methionine-R-sulfoxide reductase from *Saccharomyces cerevisiae*. *J. Biol. Chem.* 284,  
634 4354–4364. <https://doi.org/10.1074/jbc.M805891200>
- 635 Lin, Z., Johnson, L.C., Weissbach, H., Brot, N., Lively, M.O., Lowther, W.T., 2007. Free  
636 methionine-(R)-sulfoxide reductase from *Escherichia coli* reveals a new GAF domain  
637 function. *Proc. Natl. Acad. Sci. U. S. A.* 104, 9597–9602.  
638 <https://doi.org/10.1073/pnas.0703774104>
- 639 Loschi, L., Brokx, S.J., Hills, T.L., Zhang, G., Bertero, M.G., Lovering, A.L., Weiner, J.H.,  
640 Strynadka, N.C.J., 2004. Structural and Biochemical Identification of a Novel  
641 Bacterial Oxidoreductase. *J. Biol. Chem.* 279, 50391–50400.  
642 <https://doi.org/10.1074/jbc.M408876200>
- 643 Lowther, W.T., Weissbach, H., Etienne, F., Brot, N., Matthews, B.W., 2002. The mirrored  
644 methionine sulfoxide reductases of *Neisseria gonorrhoeae* pilB. *Nat. Struct. Biol.* 9,  
645 348–352. <https://doi.org/10.1038/nsb783>
- 646 Luo, S., Levine, R.L., 2009. Methionine in proteins defends against oxidative stress. *FASEB*  
647 *J. Off. Publ. Fed. Am. Soc. Exp. Biol.* 23, 464–472. <https://doi.org/10.1096/fj.08-118414>
- 648
- 649 Madeira, J.-P., Alpha-Bazin, B.M., Armengaud, J., Duport, C., 2017. Methionine Residues in  
650 Exoproteins and Their Recycling by Methionine Sulfoxide Reductase AB Serve as an  
651 Antioxidant Strategy in *Bacillus cereus*. *Front. Microbiol.* 8, 1342.  
652 <https://doi.org/10.3389/fmicb.2017.01342>
- 653 Melnyk, R.A., Youngblut, M.D., Clark, I.C., Carlson, H.K., Wetmore, K.M., Price, M.N.,  
654 Iavarone, A.T., Deutschbauer, A.M., Arkin, A.P., Coates, J.D., 2015. Novel



- 655 mechanism for scavenging of hypochlorite involving a periplasmic methionine-rich  
656 Peptide and methionine sulfoxide reductase. *mBio* 6, e00233-00215.  
657 <https://doi.org/10.1128/mBio.00233-15>
- 658 Messner, K.R., Imlay, J.A., 1999. The identification of primary sites of superoxide and  
659 hydrogen peroxide formation in the aerobic respiratory chain and sulfite reductase  
660 complex of *Escherichia coli*. *J. Biol. Chem.* 274, 10119–10128.
- 661 Moskovitz, J., Singh, V.K., Requena, J., Wilkinson, B.J., Jayaswal, R.K., Stadtman, E.R.,  
662 2002. Purification and characterization of methionine sulfoxide reductases from  
663 mouse and *Staphylococcus aureus* and their substrate stereospecificity. *Biochem.*  
664 *Biophys. Res. Commun.* 290, 62–65. <https://doi.org/10.1006/bbrc.2001.6171>
- 665 Prentki, P., Krisch, H.M., 1984. In vitro insertional mutagenesis with a selectable DNA  
666 fragment. *Gene* 29, 303–313.
- 667 Quandt, J., Hynes, M.F., 1993. Versatile suicide vectors which allow direct selection for gene  
668 replacement in gram-negative bacteria. *Gene* 127, 15–21.
- 669 Ray, S.S., Singh, S.K., Balaram, P., 2001. An electrospray ionization mass spectrometry  
670 investigation of 1-anilino-8-naphthalene-sulfonate (ANS) binding to proteins. *J. Am.*  
671 *Soc. Mass Spectrom.* 12, 428–438. [https://doi.org/10.1016/S1044-0305\(01\)00206-9](https://doi.org/10.1016/S1044-0305(01)00206-9)
- 672 Sabaty, M., Grosse, S., Adryanczyk, G., Boiry, S., Biaso, F., Arnoux, P., Pignol, D., 2013.  
673 Detrimental effect of the 6 His C-terminal tag on YedY enzymatic activity and  
674 influence of the TAT signal sequence on YedY synthesis. *BMC Biochem.* 14, 28.  
675 <https://doi.org/10.1186/1471-2091-14-28>
- 676 Saleh, M., Bartual, S.G., Abdullah, M.R., Jensch, I., Asmat, T.M., Petruschka, L., Pribyl, T.,  
677 Gellert, M., Lillig, C.H., Antelmann, H., Hermoso, J.A., Hammerschmidt, S., 2013.  
678 Molecular architecture of *Streptococcus pneumoniae* surface thioredoxin-fold  
679 lipoproteins crucial for extracellular oxidative stress resistance and maintenance of  
680 virulence. *EMBO Mol. Med.* 5, 1852–1870.  
681 <https://doi.org/10.1002/emmm.201202435>
- 682 Sharov, V.S., Ferrington, D.A., Squier, T.C., Schöneich, C., 1999. Diastereoselective  
683 reduction of protein-bound methionine sulfoxide by methionine sulfoxide reductase.  
684 *FEBS Lett.* 455, 247–250.
- 685 Skaar, E.P., Tobiason, D.M., Quick, J., Judd, R.C., Weissbach, H., Etienne, F., Brot, N.,  
686 Seifert, H.S., 2002. The outer membrane localization of the *Neisseria gonorrhoeae*  
687 MsrA/B is involved in survival against reactive oxygen species. *Proc. Natl. Acad. Sci.*  
688 *U. S. A.* 99, 10108–10113. <https://doi.org/10.1073/pnas.152334799>
- 689 Tarrago, L., Gladyshev, V.N., 2012. Recharging oxidative protein repair: catalysis by  
690 methionine sulfoxide reductases towards their amino acid, protein, and model  
691 substrates. *Biochem. Biokhimiia* 77, 1097–1107.  
692 <https://doi.org/10.1134/S0006297912100021>
- 693 Tarrago, L., Kaya, A., Weerapana, E., Marino, S.M., Gladyshev, V.N., 2012. Methionine  
694 sulfoxide reductases preferentially reduce unfolded oxidized proteins and protect cells  
695 from oxidative protein unfolding. *J. Biol. Chem.* 287, 24448–24459.  
696 <https://doi.org/10.1074/jbc.M112.374520>
- 697 Vieira Dos Santos, C., Cuiné, S., Rouhier, N., Rey, P., 2005. The Arabidopsis plastidic  
698 methionine sulfoxide reductase B proteins. Sequence and activity characteristics,  
699 comparison of the expression with plastidic methionine sulfoxide reductase A, and  
700 induction by photooxidative stress. *Plant Physiol.* 138, 909–922.  
701 <https://doi.org/10.1104/pp.105.062430>
- 702 Vogt, W., 1995. Oxidation of methionyl residues in proteins: tools, targets, and reversal. *Free*  
703 *Radic. Biol. Med.* 18, 93–105.

- 704 Weiner, J.H., MacIsaac, D.P., Bishop, R.E., Bilous, P.T., 1988. Purification and properties of  
705 Escherichia coli dimethyl sulfoxide reductase, an iron-sulfur molybdoenzyme with  
706 broad substrate specificity. *J. Bacteriol.* 170, 1505–1510.
- 707 Winter, J., Ilbert, M., Graf, P.C.F., Ozelik, D., Jakob, U., 2008. Bleach activates a redox-  
708 regulated chaperone by oxidative protein unfolding. *Cell* 135, 691–701.  
709 <https://doi.org/10.1016/j.cell.2008.09.024>
- 710 Ziegelhoffer, E.C., Donohue, T.J., 2009. Bacterial responses to photo-oxidative stress. *Nat.*  
711 *Rev. Microbiol.* 7, 856–863. <https://doi.org/10.1038/nrmicro2237>  
712

713 **Table 1.** Kinetics parameters of RsMsrP reductase activity towards various MetO-containing  
714 substrates.

| <b>Substrates</b>            | <b><math>k_{cat}</math> (<math>s^{-1}</math>)</b> | <b><math>K_M</math><br/>(<math>\mu M</math>)</b> | <b><math>k_{cat}/K_M</math><br/>(<math>M^{-1}.s^{-1}</math>)</b> |
|------------------------------|---|--|--|
| DMSO <sup>a</sup>            | 28 ± 1  | 61,000 ± 7,000                                   | 465  |
| Free L-Met- <i>R,S</i> -O    | 122 ± 20  | 115,000 ± 27,000                                 | 1,000  |
| Ser-MetO-Ser                 | 108 ± 17  | 13,000 ± 3,400                                   | 8,300  |
| QWGAGM(O)QAEED               | 479 ± 24  | 4,530 ± 370                                      | 105,700  |
| TTPGYM(O)EEWNK               | > 70  | > 5,000  | N.D.   |
| Oxidized $\beta$ -casein     | 100 ± 5   | 93 ± 9   | 1,075,000  |
| $\beta$ -casein- <i>R</i> -O | 49 ± 3  | 51 ± 6   | 950,000  |
| $\beta$ -casein- <i>S</i> -O | 8 ± 1   | 53 ± 10  | 142,000  |
| Oxidized lysozyme            | 4 ± 1   | 886 ± 349  | 4,000  |
| Unfolded oxidized lysozyme   | 7 ± 1   | 105 ± 17   | 70,200   |
| Oxidized GST                 | 8 ± 2   | 643 ± 194  | 12,400   |
| Unfolded oxidized GST        | 12 ± 3  | 99 ± 33  | 120,000  |

715 <sup>a</sup> From [Sabaty et al., 2013](#). *N.D.*, not determined.

716

## 717 **Materials and methods**

### 718 *Production and purification of recombinant proteins*

719           Recombinant MsrP was produced similarly as described in (Sabaty et al., 2013). Briefly,  
720 *R. sphaeroides* f sp. *denitrificans* IL106 *dmsA*<sup>-</sup> strain carrying pSM189 plasmid allowing the  
721 production of a periplasmic MsrP with a 6-His N-terminal tag was grown in 6-liter culture under  
722 semi-aerobic conditions in Hutner medium until late exponential phase. Periplasmic fraction  
723 was extracted and loaded on HisTrap column (GE Healthcare) then MsrP was eluted by an  
724 imidazole step gradient. MsrP solution was concentrated using 15-ml Amicon<sup>®</sup> Ultra  
725 concentrators with 10-kDa cutoff (Millipore), desalted with Sephadex G-25 in PD-10 Desalting  
726 Columns (GE Healthcare). The protein concentration was adjusted to 1 mg.ml<sup>-1</sup> in Tris-HCl 30  
727 mM, 500 mM NaCl, pH 7.5, the Tobacco Etch Virus (TEV) protease was added (1:80  
728 TEV:RsMsrP mass ratio) and the solution incubated overnight at room temperature to remove  
729 the polyhistidine tag. Untagged RsMsrP was purified on a second HisTrap column, then  
730 concentrated and desalted in 50 mM 4-(2-hydroxyethyl)-1-piperazineethanesulfonic acid  
731 (HEPES), pH 8.0. Protein solution was then loaded on gel filtration in Superdex<sup>™</sup> 200 10/30  
732 column equilibrated with Tris-HCl 30 mM, pH 7.5. Main fractions were pooled and applied to  
733 a MonoQ<sup>™</sup> 4.6/100 PE (GE Healthcare). RsMsrP was then eluted using a linear NaCl gradient  
734 (0 to 500 mM). Fractions were analyzed on SDS-PAGE using NuPAGE<sup>™</sup>, 10 % Bis-Tris gels  
735 with MES-SDS buffer (ThermoFisher). Recombinant MsrA, MsrB, Thioredoxin Reductase  
736 (TR) 1, Thioredoxin 1 (Trx1) from *Saccharomyces cerevisiae* and containing a polyhistidine  
737 tag, as well as the glutathione-S-transferase (GST) from *Schistosoma japonicum*, were  
738 produced and purified as previously described (Tarrago et al., 2012). Protein concentrations  
739 were determined spectrophotometrically using specific molar extinction coefficients at 280 nm:  
740 6-His-RsMSRP, 56,380 M<sup>-1</sup>.cm<sup>-1</sup>; untagged RsMsrP, 54,890 M<sup>-1</sup>.cm<sup>-1</sup>; MsrA, 34,630 M<sup>-1</sup>.cm<sup>-1</sup>;  
741 MsrB, 24,325 M<sup>-1</sup>.cm<sup>-1</sup>; TR1, 24,410 M<sup>-1</sup>.cm<sup>-1</sup>; Trx1, 9,970 M<sup>-1</sup>.cm<sup>-1</sup>; GST, 42,860 M<sup>-1</sup>.cm<sup>-1</sup>,

742 bovine  $\beta$ -casein (Sigma-Aldrich),  $11,460 \text{ M}^{-1}.\text{cm}^{-1}$  and chicken lysozyme (Sigma-Aldrich),  
743  $32,300 \text{ M}^{-1}.\text{cm}^{-1}$ . Protein solutions were stored at  $-20^\circ\text{C}$  until further use.

744

#### 745 *Peptides*

746 Ser-Met(O)-Ser, QWGAGM(O)QAEED and TTPGYM(O)EEWNK peptides were obtained  
747 from GenScript® (Hong-Kong).

748

#### 749 *Preparation of oxidized bovine $\beta$ -casein and its Met-R-O and Met-S-O containing counterparts*

750 For oxidation, bovine  $\beta$ -casein was incubated in Phosphate Buffer Saline (PBS) at 1  
751  $\text{mg}.\text{ml}^{-1}$  in the presence of 200 mM  $\text{H}_2\text{O}_2$  and incubated overnight at room temperature.  $\text{H}_2\text{O}_2$   
752 was removed by desalting using PD-10 column and the protein solution was concentrated with  
753 10-kDa cutoff Amicon® Ultra concentrator. Oxidized GST was prepared similarly using 100  
754 mM  $\text{H}_2\text{O}_2$ . To prepare Met-R-O containing  $\beta$ -casein, a solution of oxidized  $\beta$ -casein was  
755 incubated in Tris-HCl 30 mM, pH 8 at a final concentration of  $6.5 \text{ mg}.\text{ml}^{-1}$  ( $260 \mu\text{M}$ ) in the  
756 presence of 25 mM dithiothreitol (DTT) and  $10 \mu\text{M}$  MsrA and incubated overnight at room  
757 temperature. The solution was 10-fold diluted in Tris-HCl 30 mM, pH 8 and passed on HisTrap  
758 column to remove the his-tagged MsrA. After concentration, the DTT was removed by  
759 desalting using PD-10 column. Met-S-O containing  $\beta$ -casein was prepared similarly replacing  
760 the MsrA by the MsrB ( $14 \mu\text{M}$ ). The protein solutions were concentrated with 10-kDa cutoff  
761 Amicon® Ultra concentrator and the final concentration was determined  
762 spectrophotometrically. Protein solutions were stored at  $-20^\circ\text{C}$  until further use.

763

764 *Enzymatic activity and apparent stoichiometry measurements*

765 RsMsrP reductase activity was measured as described in (Sabaty et al., 2013) with few  
766 modifications. Benzyl viologen was used as electron donor and its consumption was followed  
767 at 600 nm using at UVmc1<sup>®</sup> spectrophotometer (SAFAS Monaco) equipped with optic fibers  
768 in a glovebox workstation (MBRAUN Labstar) flushed with nitrogen. We determined the  
769 specific molar extinction coefficient of benzyl viologen at 8,700 M<sup>-1</sup>.cm<sup>-1</sup> in 50 mM 2-(*N*-  
770 morpholino)ethanesulfonic acid (MES), pH 6.0 buffer. Each reaction mixture (1 ml or 0.5 ml)  
771 contained 0.2 mM benzyl viologen reduced with sodium dithionite, and variable concentrations  
772 of substrates in 50 mM MES, pH 6.0 buffer.

773 Reactions were started by addition of the RsMsrP enzyme (10 to 46 nM). Reduction of  
774 MetO rates were calculated from  $\Delta A_{600\text{ nm}}$  slopes respecting a stoichiometry of 2 (2 moles of  
775 benzyl viologen are oxidized for 1 mole of MetO reduced).

776 The apparent stoichiometry was determined similarly, using subsaturating  
777 concentrations of substrates: 1–10  $\mu\text{M}$  oxidized  $\beta$ -casein, 1–10  $\mu\text{M}$  Met-*R*-O containing  
778  $\beta$ -casein and 1.5–15  $\mu\text{M}$  Met-*S*-O containing  $\beta$ -casein. The amount of oxidized benzyl viologen  
779 was determined 1 hour after the addition of the RsMsrP (46 nM) by subtracting the final  $A_{600}$   
780 nm value to the initial one. Controls were made without the RsMsrP enzyme, and without the  
781 MetO-containing substrate. Quantities of MetO reduced were plotted as function of substrates  
782 quantities and the apparent stoichiometry was obtained from the slope of the linear regression.

783 MsrA and MsrB activities were measured following the consumption of NADPH  
784 spectrophotometrically at 340 nm using the thioredoxin system similarly as previously  
785 described (Tarrago et al., 2012). A 500- $\mu\text{l}$  reaction cuvette contained 200  $\mu\text{M}$  NADPH, 2  $\mu\text{M}$   
786 TR1, 25  $\mu\text{M}$  Trx1 and 5  $\mu\text{M}$  MsrA or MsrB and 100  $\mu\text{M}$  oxidized  $\beta$ -casein. Production of Met  
787 was calculated respecting a stoichiometry of 1 (1 mole of NADPH is oxidized for 1 mole of  
788 Met produced).

789 Analysis and kinetics parameters determination were made using GraphPad® Prism 4.0  
790 software (La Jolla, CA, USA).

791

792 *Electrospray ionization/Mass spectrometry analysis of purified proteins*

793 For oxidation, bovine  $\beta$ -casein (5 mg.ml<sup>-1</sup>) in 50 mM HEPES, pH 7.0, was incubated overnight  
794 at room temperature with H<sub>2</sub>O<sub>2</sub> (50 mM). H<sub>2</sub>O<sub>2</sub> was removed by desalting using PD-10 column  
795 and the protein solution was concentrated with 10-kDa cutoff Amicon® Ultra concentrator.  
796 Oxidized  $\beta$ -casein (100  $\mu$ M) was reduced by addition of 44 nM MsrP in a reaction mixture  
797 containing 50 mM HEPES pH 7.0, 0.8 mM benzyl viologen and 0.2 mM sodium dithionite.  
798 After two hours reaction in the glove-box, the repaired  $\beta$ -casein was analyzed by mass  
799 spectrometry in comparison to non-oxidized and oxidized  $\beta$ -casein.

800 Mass spectrometry analyses were performed on a MicroTOF-Q Bruker (Wissembourg, France)  
801 with an electrospray ionization source. Samples were desalted and concentrated in ammonium  
802 acetate buffer (20 mM) (Sigma-Aldrich) prior analyses with Centricon Amicon (Millipore) with  
803 a cutoff of 30 kDa. Samples were diluted with CH<sub>3</sub>CN/H<sub>2</sub>O (1/1-v/v), 0.2% Formic Acid  
804 (Sigma). Samples were continuously infused at a flow rate of 3  $\mu$ L/min. Mass spectra were  
805 recorded in the 50-7000 mass-to-charge (m/z) range. MS experiments were carried out with a  
806 capillary voltage set at 4.5 kV and an end plate off set voltage at 500 V. The gas nebulizer (N<sub>2</sub>)  
807 pressure was set at 0.4 bars and the dry gas flow (N<sub>2</sub>) at 4 L/min at a temperature of 190 °C.  
808 Data were acquired in the positive mode and calibration was performed using a calibrating  
809 solution of ESI Tune Mix (Agilent) in CH<sub>3</sub>CN/H<sub>2</sub>O (95/5-v/v). The system was controlled with  
810 the software package MicroTOF Control 2.2 and data were processed with DataAnalysis 3.4.

811

812 *Generation of R. sphaeroides 2.4.1 msrP<sup>-</sup> mutant*

813 The *msrPQ* operon was amplified from *R. sphaeroides* 2.4.1 genomic DNA with the primers  
814 5'-AGATCGACACGCCATTCACC-3' and 5'-TCGGTGAGGCGCTATCTAGG-3'. The 2.2  
815 kb PCR product was cloned into pGEMT Easy (Promega). An omega cartridge encoding  
816 resistance to streptomycin and spectinomycin (Prentki and Krisch, 1984) was then cloned into  
817 the *Bam*HI site of *msrP*. The resulting plasmid was digested with *Sac*I and the fragment  
818 containing the disrupted *msrP* gene was cloned into pJQ200mp18 (Quandt and Hynes, 1993).  
819 The obtained plasmid, unable to replicate in *R. sphaeroides*, was transferred from *E. coli* by  
820 conjugation. The occurrence of a double-crossing over event was confirmed by PCR and  
821 absence of the protein from the SDS-PAGE profile.

822

#### 823 *Preparation of periplasmic samples for proteomics analysis*

824 *R. sphaeroides* 2.4.1 *msrP*<sup>-</sup> mutant was grown under semi-aerobic conditions. Periplasmic  
825 extract was prepared as previously described (Sabaty et al., 2010) by cells incubation in 50 mM  
826 HEPES pH 8.0, 0.45 M sucrose, 1.3 mM Ethylenediaminetetraacetic acid (EDTA) and 1  
827 mg.ml<sup>-1</sup> chicken lysozyme. For Met oxidation, the periplasmic extract (0.7 mg.ml<sup>-1</sup>) was  
828 incubated with 20 mM *N*-Ethylmaleimide (NEM) and 2 mM NaOCl (Sigma-Aldrich) in 50 mM  
829 HEPES pH 8.0, 50 mM NaCl for 10 min at room temperature. NaOCl was removed by desalting  
830 using PD-10 column and buffer was changed for 50 mM MES pH 6.0. The protein solution was  
831 concentrated with 3-kDa cutoff Amicon<sup>®</sup> Ultra concentrator. Three reaction mixtures were  
832 prepared in the glove box containing 35 µl of periplasmic extract, 1 mM benzyl viologen, 2  
833 mM dithionite in 50 mM MES pH 6.0. The protein concentration in each reaction was 2.5  
834 mg.ml<sup>-1</sup>. The first reaction contained non-oxidized periplasmic extract, the second and third  
835 ones contained oxidized periplasmic extract. For the third reaction (repaired periplasm) 10 µM  
836 RsMsrP was added. The reactions were incubated for three hours at room temperature.



837

838 *Trypsin proteolysis and tandem mass spectrometry*

839 Protein extracts were immediately subjected to denaturing PAGE electrophoresis for 5 min onto  
840 a 4–12% gradient 10-well NuPAGE (Invitrogen) gel. The proteins were stained with Coomassie  
841 Blue Safe solution (Invitrogen). Polyacrylamide bands corresponding to the whole proteomes  
842 were sliced and treated with iodoacetamide and then trypsin as previously recommended by  
843 (Hartmann et al., 2014). Briefly, each band was destained with ultra-pure water, reduced with  
844 dithiothreitol, treated with iodoacetamide, and then proteolyzed with Trypsin Gold Mass  
845 Spectrometry Grade (Promega) in the presence of 0.01% ProteaseMAX surfactant (Promega).  
846 Peptides were immediately subjected to tandem mass spectrometry as previously recommended  
847 to avoid methionine oxidation (Madeira et al., 2017). The resulting peptide mixtures were  
848 analyzed in a data-dependent mode with a Q-Exactive HF tandem mass spectrometer (Thermo)  
849 coupled on line to an Ultimate 3000 chromatography system chromatography (Thermo)  
850 essentially as previously described (Klein et al., 2016). A volume of 10  $\mu$ L of each peptide  
851 sample was injected, first desalted with a reverse-phase Acclaim PepMap 100 C18 (5  $\mu$ m, 100  
852  $\text{\AA}$ , 5 mm x 300  $\mu$ m i.d., Thermo) precolumn and then separated at a flow rate of 0.2  $\mu$ L per min  
853 with a nanoscale Acclaim PepMap 100 C18 (3  $\mu$ m, 100  $\text{\AA}$ , 500 mm x 300  $\mu$ m i.d., Thermo)  
854 column using a 150 min gradient from 2.5 % to 25 % of  $\text{CH}_3\text{CN}$ , 0.1% formic acid, followed  
855 by a 30 min gradient from 25% to 40% of  $\text{CH}_3\text{CN}$ , 0.1% formic acid. Mass determination of  
856 peptides was done at a resolution of 60,000. Peptides were then selected for fragmentation  
857 according to a Top20 method with a dynamic exclusion of 10 sec. MS/MS mass spectra were  
858 acquired with an AGC target set at  $1.7 \cdot 10^5$  on peptides with 2 or 3 positive charges, an isolation  
859 window set at 1.6  $m/z$ , and a resolution of 15,000.

860

861 *MS/MS spectrum assignment, peptide validation and protein identification*

862 Peak lists were automatically generated from raw datasets with Proteome Discoverer 1.4.1  
863 (Thermo) and an in-house script with the following options: minimum mass (400), maximum  
864 mass (5,000), grouping tolerance (0), intermediate scans (0) and threshold (1,000). The  
865 resulting .mgf files were queried with the Mascot software version 2.5.1 (Matrix Science)  
866 against the *R. sphaeroides* 241 annotated genome database with the following parameters: full-  
867 trypsin specificity, up to 2 missed cleavages allowed, static modification of  
868 carbamidomethylated cysteine, variable oxidation of methionine, variable deamidation of  
869 asparagine and glutamine, mass tolerance of 5 ppm on parent ions and mass tolerance on  
870 MS/MS of 0.02 Da. The decoy search option of Mascot was activated for estimating the false  
871 discovery rate (FDR) that was below 1%. Peptide matches with a MASCOT peptide score  
872 below a p value of 0.05 were considered. Proteins were validated when at least two different  
873 peptides were detected. The FDR for proteins was below 1% as estimated with the MASCOT  
874 reverse database decoy search option.

875

876 *Ice logo analysis*

877 Ice logoanalysis were performed using the IceLogo server  
878 (<http://iomics.ugent.be/icelogoserver/index.html>) (Colaert et al., 2009).